

# Towards deep learning-based wall shear stress prediction for intracranial aneurysms

Annika Niemann<sup>1,2</sup>, Lisa Schneider<sup>1</sup>, Bernhard Preim<sup>1</sup>, Samuel Voß<sup>2,3</sup>,  
Philipp Berg<sup>2,3</sup>, Sylvia Saalfeld<sup>1,2</sup>

<sup>1</sup>Department of Simulation and Graphics, Otto-von-Guericke University of  
Magdeburg

<sup>2</sup>Forschungscampus *STIMULATE*, Otto-von-Guericke University of Magdeburg

<sup>3</sup>Department of Fluid Dynamics and Technical Flows, University of Magdeburg

`annika.niemann@ovgu.de`

**Abstract.** This work aims at a deep learning-based prediction of wall shear stresses (WSS) for intracranial aneurysms. Based on real patient cases, we created artificial surface models of bifurcation aneurysms. After simulation and WSS extraction, these models were used for training a deep neural network. The trained neural network for 3D mesh segmentation was able to predict areas of high wall shear stress.

## 1 Introduction

Intracranial aneurysm growth and rupture is strongly associated with the blood flow inside the aneurysm and its parent vessel. Assessment of individual rupture risk can be supported by hemodynamic simulations [1]. These are time-consuming and need expert knowledge. For the integration of wall shear stress (WSS) information into clinical routine a deep learning method might be used. In this work we explore how areas of high wall shear stress can be predicted using deep learning on surface meshes.

Recently, Gharleghi et al. [2] presented deep learning WSS prediction for the left main coronary artery bifurcation. They splitted the bifurcation into separate vessels. For each part, a 2D representation with several geometrical parameters was generated. Then, deep learning was applied to the 2D representation. Their results had an average mean absolute error of 0.0407 Pa.

Based on 4000 artificially created abdominal aortic aneurysms, Jordanski et al. [3] compared several machine learning approaches to model the relationship between geometric parameters and WSS distribution. The best results were achieved by Gaussian conditional random fields. In this study we generated artificial intracranial aneurysms and performed deep learning mesh segmentation to predict areas of high WSS.

**Table 1.** Parameters of real world aneurysms that were characterised by a roundly shaped saccular aneurysm at vessel bifurcation. Provided are min, max and average values (in degree respectively mm) for the parameters described in Fig. 1

	$r_i$	$r_1$	$r_2$	$r_a$	$d$	$\alpha$	$\beta$
average	2.53	1.87	1.75	2.09	3.67	97.31	93.77
min	1.81	0.96	1.04	1.11	1.65	64.00	60.00
max	3.38	2.48	2.58	3.44	6.15	157.00	120.00

## 2 Materials and methods

For this study we chose a simplified configuration consisting of a bifurcation aneurysm with one inlet and two outlets of the parent artery. Based on the results of hemodynamic simulations, regions of high WSS were segmented and serve as ground truth.

### 2.1 Artificial aneurysm configuration

The simplified, artificial bifurcation aneurysms were created with CAD software. Each geometry consists of three cylinders, representing one inlet vessel and two outlets and a sphere for the saccular bifurcation aneurysm. The aneurysm creation has seven adjustable parameters (see Fig. 1): the radius of the inlet ( $r_i$ ), the radius of the first outlet ( $r_1$ ), the radius of the second outlet ( $r_2$ ), the radius of the aneurysm ( $r_a$ ), the distance between aneurysm center and bifurcation ( $d$ ), the angle between the first outlet and the inlet ( $\alpha$ ), and the angle between the second outlet and the inlet ( $\beta$ ). In order to extract realistic default values for these parameters, we analyzed 200 patient-specific 3D aneurysm models from our previous work. We then selected cases which have a high agreement w.r.t. our artificial configuration (i.e. spherical, saccular bifurcation aneurysm) yielding 13 reference cases. Their average, minimum and maximum values are shown in Table 1. The artificial aneurysms were created with randomly generated parameters in the same range of the values of the reference aneurysms.

### 2.2 Hemodynamic simulations

Hemodynamic simulations were performed in order to assess the WSS of the artificial aneurysm geometries. These simulations are based on computational fluid dynamics, which is a numerical approach to solve fluid flow problems using Navier-Stokes equations. For this purpose, each flow domain, containing vessels and aneurysm, was spatially discretized into volumetric cells (1.2 to 2.4 million cells for each configuration depending on the domain size). Blood was modeled as incompressible and laminar fluid with a density of  $1055 \text{ kg/m}^3$  and dynamic viscosity of  $0.004 \text{ Pa}\cdot\text{s}$ . Boundary conditions of the domain were modeled as follows: Constant velocity of  $0.3 \text{ m/s}$  as inflow into the parent artery, rigid vessel walls with no-slip condition, and zero-pressure assumption at the outlets. The total simulation time was  $5 \text{ s}$  (quasi-steady, time step of  $0.01 \text{ s}$ ) while only the time

range of [3-5] s was used for temporal averaging the WSS field. In total, 145 artificial aneurysms were simulated with STAR-CCM+ 13.06 (Siemens PLM Software Inc., Plano, TX, USA). Finally, aneurysm surface and temporal averaged WSS magnitude values were exported for further analysis.

### 2.3 Deep learning segmentation

The aneurysm surfaces are remeshed using the ACVD algorithm [4] to obtain a similar number of edges. The deep learning approach requires label per edge while the WSS magnitude values from the flow simulation were obtained at vertices. Thus, we calculate the edge labels as average WSS of the associated vertices. Areas of high WSS are defined based on a reference value. This reference value is obtained by listing the maximum WSS of each aneurysm and calculating the median of it. Areas, where the WSS is larger than 0.4 times the reference value, are defined as areas of high WSS. An example is shown in Figure 2.

We trained a deep learning mesh segmentation using the *medMeshCNN* architecture [5]. For the first experiment, we used a small dataset consisting of 24 training meshes and 3 test meshes. The second experiment included 123 training and 10 test meshes. Due to problems in feature calculation, the last experiment comprised 118 training and 9 test meshes.

Instead of transforming the mesh information to 2D, we directly work with 3D surface meshes. Deep learning segmentation is used to predict areas of high WSS. Further experiments included variation of the edge features used. *medMeshCNN* calculates angles and ratio between edges of adjacent faces. In experiments 3,4 and 5 we added curvature [6] and in experiment 5 mesh thickness [7] (defined as diameter of the maximum inscribed sphere) to the feature calculation. Both features were first calculated for each vertex and then mapped to the corresponding

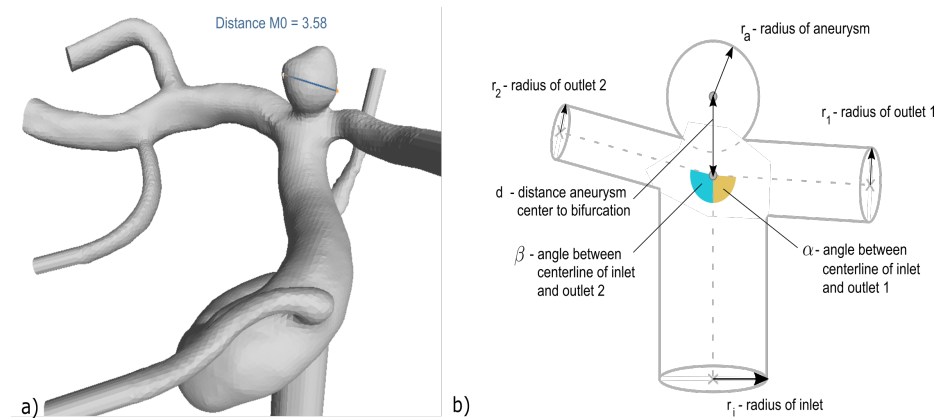


**Fig. 1.** Overview of parameters for artificial aneurysm creation; a) example of reference aneurysm with measure of aneurysm diameter; b) concept of artificial aneurysm creation with seven parameters.

**Table 2.** Parameters of the experiments, where # denotes the experiment number, *GC* the Gaussian curvature and *MC* the mean Gaussian curvature.

#	training	test	additional features	pooling resolution	batch size	weighted loss
1	15	3	-	2500 2000 1500 1000 750	10	0.2 0.8
2	123	10	-	2500 2000 1500 1000 750	10	0.2 0.8
3	123	10	<i>GC</i>	2500 2000 1500 1000 750	10	0.2 0.8
4	123	10	<i>GC</i> & <i>MC</i>	2500 2000 1500 1000 750 500	5	0.01 0.99
5	118	9	<i>GC</i> & thickness	2500 2000 1500 1000 750 500	5	0.01 0.99

edges. In the following, selected experiments are presented. The parameters of each experiment are summarised in Table 2.

### 3 Results

The training accuracy of the first experiment was constantly increasing and approaching 100%. This proved that the *medMeshCNN* architecture is able to learn the presented mesh attributes. However, the test accuracy was far worse (between 61 and 68%) and decreasing after 50 epochs.

Increasing the number of training meshes did improve the test accuracy, as shown by the second experiment (see Fig. 3). Again, overfitting occurred and the test accuracy decreased after epoch 40. In Figure 4, the result for one of the test meshes is shown. The corresponding simulation result and ground truth are shown in Figure 2. While an accuracy over 85% is reached, the visual inspection shows some differences. Only a small part of the large WSS area is predicted by the net. But additional spots on the wall are falsely predicted.

For the third experiment the Gaussian curvature was included in the feature list. As visible in Figure 3, this leads to a test accuracy of over 91%. Unfortunately, this accuracy was reached by labelling most edges as normal WSS, omitting the high WSS class.

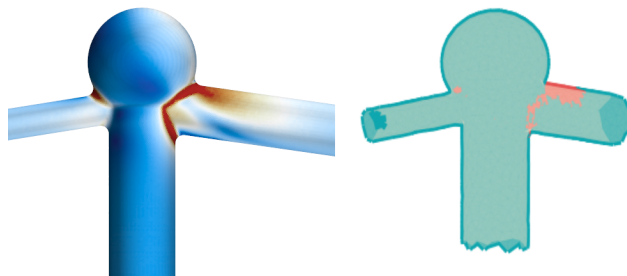


**Fig. 2.** Depiction of the resulting WSS (left) and a corresponding ground truth segmentation for training (right).

To overcome the problem of the vanishing high WSS class, the weights of the loss function were adjusted. Experiment 4 additionally included the mean Gaussian curvature as a feature. Thus, an accuracy of 85% was reached (compare Fig. 3). Figure 4 shows the prediction of the net. Compared to experiment 2, there are less but larger predicted high WSS areas. The net from experiment 4 predicts a larger area as high WSS than the ground truth segmentation for the deep learning shows. Compared with the original simulation result, both areas of high WSS are segmented by the net. The high WSS in the larger vessel is not completely segmented.

In experiment 5, additional to the curvature features, the mesh thickness was included. This did not improve the results. The test accuracy stayed below 80% and WSS areas were scattered over the whole mesh (see Fig. 4).

Prediction of high WSS areas with the trained net needed 43 seconds on average per mesh.

## 4 Discussion

Areas of high WSS can be predicted by deep learning mesh segmentation methods. In all presented experiments, the training accuracy converged to 100%.

While high training accuracy was reached, the test accuracy showed limitations. A major limitation is the used dataset. As seen in the first two experiments, increasing the number of training examples does improve the test accuracy. We used artificially created intracranial aneurysms. These shared the same basic geometry, a bifurcation aneurysm with proximal parent and two distal outflow vessels. *medMeshCNN* is able to learn the geometry based on meshes and mesh features. While the geometries of the meshes are similar, the variance in the

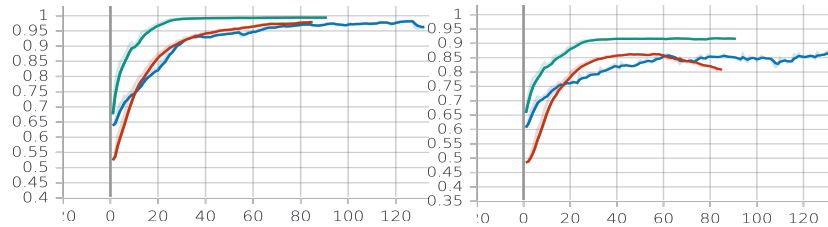


**Fig. 3.** Training (left) and test (right) accuracy per epoch of experiment 2 (without additional features; red), experiment 3 (GC; green), experiment 4 (GC&MC; blue).

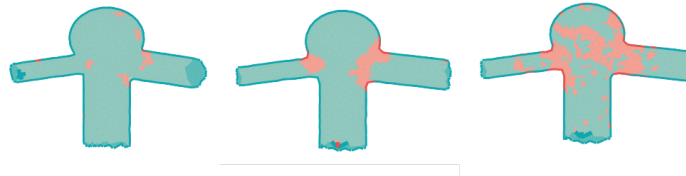


**Fig. 4.** Result of experiment 2 (left), 4 (middle) and 5 (right).

segmentation is higher. This might hinder the training and complicate generalization. Including the curvature and adjusting the weights of the loss function does improve the results.

Another factor which needs further research is the choice of suitable thresholds for generation of the segmentation ground truth data. In experiment 4, a larger high WSS area around the junction was predicted than shown in the ground truth. A modified threshold value (lower reference value) might result in a better agreement between ground truth segmentation, deep learning high WSS prediction and simulation results.

In the presented work, only two WSS classes were segmented. Further research should include several classes to produce more detailed WSS predictions. Increasing the number of classes also requires careful adjustment of the training parameters, especially the weights for the loss function.

While finding suitable parameters for the net is a challenging and time-consuming task, the prediction of WSS with deep learning is considerably faster than traditional hemodynamic simulation and does not require expert knowledge.

In conclusion, we analyzed the potential of deep learning mesh segmentation for the fast prediction of WSS in intracranial bifurcation aneurysms. This approach provides fast results, which could be included into clinical routine. The quality of the results depends on several parameters. A weighted loss function with focus on the high WSS areas and the inclusion of the mesh curvature improved the prediction results.

## References

1. Berg P, Voß S, Janiga G, et al. Multiple Aneurysms AnaTomy CHallenge 2018 (MATCH)—phase II: rupture risk assessment. *Int J Comput Assist Radiol Surg.* 2019 05;14.
2. Gharleghi R, Samarasinghe G, Sowmya A, et al. Deep Learning for Time Averaged Wall Shear Stress Prediction in Left Main Coronary Bifurcations. In: 2020 IEEE 17th International Symposium on Biomedical Imaging (ISBI); 2020. p. 1–4.
3. Jordanski M, Radovic M, Milosevic Z, et al. Machine Learning Approach for Predicting Wall Shear Distribution for Abdominal Aortic Aneurysm and Carotid Bifurcation Models. *IEEE Journal of Biomedical and Health Informatics.* 2016 12;PP:1–1.
4. Valette S, Chassery JM, Prost R. Generic Remeshing of 3D Triangular Meshes with Metric-Dependent Discrete Voronoi Diagrams. *IEEE Trans Vis Comput Graph.* 2008 03;14:369–381.
5. Schneider L, Niemann A, Beuing O, et al.. MedMeshCNN – Enabling MeshCNN for Medical Surface Models; 2020.
6. Cohen-Steiner D, Morvan JM. Restricted Delaunay Triangulations and Normal Cycle; 2003. p. 312–321.
7. Inui M, Umezu N, Shimane R. Shrinking sphere: A parallel algorithm for computing the thickness of 3D objects. *Computer-Aided Design and Applications.* 2016;13(2):199–207.